Progress In Electromagnetics Research Letters, Vol. 52, 37–43, 2015

Flexible VHF/UHF Vivaldi Antenna for Broadband Applications

Anthony Presse[1, *], Jean M. Floc'h[2], and Anne-Claude Tarot[1]

Abstract—A flexible VHF/UHF Vivaldi antenna is proposed. The antenna is realized on $600 \times 600\,\mathrm{mm}^2$ silicone substrate with a thickness of 1.5 mm. The silicone substrate is used due to its low cost, its robustness and its flexibility. The antenna has a -6 dB impedance bandwidth from 150 MHz up to 10 GHz. The measurements have shown that the bending slightly affects the impedance and the radiation patterns of the antenna. This last one is used for military applications to receive and find the source of VHF/UHF micro-wave emissions.

1. INTRODUCTION

The presented antenna is used to receive several signals in the VHF/UHF band such as the cellular networks (GSM, UMTS, LTE, ...), the airband, the Personal Radio Mobil, the marine VHF radio ... for military uses from 150 MHz up to 2 GHz. Due to its flexibility, several antennas can be loaded on a gas balloon (Fig. A1) and they are able to receive some signals or find their sources by a direction finding algorithm (goniometry). The set up of direction finding is made by an array of six antennas with the following antenna specifications: a half beamwidth around 60° in the E-plane, a significant gain and a return loss of 6 dB. The whole antenna should have the smallest dimensions that possible.

To design a directive, broadband and high gain antenna with a low thickness, the Vivaldi antenna seems to be the best candidate. The first appearance of the Vivaldi antenna shape was in 1979 by Gibson [1]. This type of antenna has an exponential aperture consequently different parts of this aperture radiate at different frequencies to provide a large operating bandwidth. Two main types of Vivaldi exist antenna: the Vivaldi notch antenna and the antipodal Vivaldi antenna. Generally a Vivaldi notch antenna is fed by microstrip-to-slotline transition [2]. This transition is a coupling between a microstrip with an open-ended stub and a slot line with a circular cavity. This transition has the particularity of being broadband [3]. Nevertheless, the authors of [4] have shown that a larger cavity improves greatly the lower frequency of the bandwidth but as the objective is to design an antenna with a bandwidth starting from 150 MHz, a large circular cavity should not appropriated to realize an antenna with reduced dimensions. Moreover the precision required for a microstrip-to-slotline transition [2] is not compatible for an antenna which will be bent. For these last reasons, the antipodal Vivaldi antenna is preferred for its simplicity in this study. The basic antipodal Vivaldi antenna, introduced by Gazit in 1988 [5], is composed of two conductive-wing-shaped parts on each face a substrate fed by a microstrip line. Langley et al. proposed [6] a balanced antipodal Vivaldi antenna to reduce the crosspolarisation affecting the unbalanced antipodal one.

2. ANTENNA DESIGN

2.1. Silicone-Based Flexible Substrates

A flexible material is required for the realization of conformal antennas. Textile fabrics [7] and organic polymers [8] are good candidates as soft substrate. Nevertheless, textiles such as felt are more fragile

Received 27 November 2014, Accepted 22 January 2015, Scheduled 11 March 2015
* Corresponding author: Anthony Presse (anthony.presse@univ-rennes1.fr).
[1] IETR, UMR CNRS 6164, University of Rennes 1, France. [2] IETR, INSA Rennes, France.

than an organic polymer which can be stretched [9]. The low dielectric constant of a textile does not permit an antenna size reduction. For these reasons, we were interested in the silicone, more especially in a silicon-based organic polymer. It presents, in particular, a suitable thermal stability and water resistivity. In this study, the silicone substrate has a thickness of 1.5 mm. It was characterized with two different methods. The first method uses two microstrip lines of different length [10] and the second method uses an open stub resonator [11]. At 400 MHz, the permittivity is found to be $\epsilon_r = 3.0$ and the loss tangent $tg\delta = 0.04$ [12].

2.2. Antenna Geometry

The broadband effect is created by an exponential aperture. Practically, the bandwidth is limited by the transition from the feeding to the exponential slot and obviously by the finite dimensions of the antenna [5]. We chose to design an unbalanced antipodal Vivaldi antenna as the thickness of the substrate is tinier than the wavelengths from 150 up to 2 GHz. Indeed, the skew E field between the two conductive parts, responsible of the cross polarization [6], is very small face to the slot dimensions. The antipodal Vivaldi antenna is composed of two conductive-wing-shaped parts on each face of the substrate. The antenna is fed by a 50 Ω microstrip line of 4 mm-width which turns into a parallel stripline. The width W_m of the ground plane decreases progressively for a smooth microstrip-to-stripline transition. Finally the parallel strip line goes to the exponential aperture. The exponential aperture shapes are respectively defined by the Equations (1), (2), (3) and (4) where $x \in [0, L_1]$. The antenna is optimized with CST Microwave Studio. A geometry of the antenna is shown in Fig. 1.

$$y_1(x) = \exp(C_1 x) + K_1 \tag{1}$$

$$C_1 = \frac{1}{L_2}\ln\left(\frac{H}{2} - K_1\right) \quad K_1 = -\left(\frac{W}{2}\right) - 1$$

$$y_2(x) = \exp(C_2 x) + K_2 \tag{2}$$

$$L_2 = aL_1 \quad C_2 = \frac{1}{L_2}\ln\left(\frac{H}{2} - K_2\right) \quad K_2 = \left(\frac{W}{2}\right) - 1$$

$$y_3(x) = \exp(C_3 x) + K_3 \tag{3}$$

$$C_3 = \frac{1}{L_2}\ln\left(\frac{H}{2} + K_3\right) \quad K_3 = \left(\frac{W}{2}\right) + 1$$

$$y_4(x) = \exp(C_4 x) + K_4 \tag{4}$$

$$C_4 = \frac{1}{L_2}\ln\left(\frac{H}{2} + K_4\right) \quad K_4 = -\left(\frac{W}{2}\right) + 1$$

Figure 2 shows the reflection coefficient of the antenna from 0.1 GHz up to 10 GHz. As it can be observed the antenna has an ultra wideband. Nevertheless we can notice that the −6 dB threshold is not reached in the lower band.

The dimensionless coefficient a ($a < 1$) allows to control the impedance in the lower band. Fig. 3 shows the influence of a on the reflection coefficient. This coefficient mainly affects the impedance matching up to 350 MHz. Precisely, the lower is a, the larger is the bandwidth. a is set at 0.15. The optimized dimensions of the antenna are summarized in Table 1.

Table 1. Optimized antenna dimensions.

Designation	Dimension		Designation	Dimension
$h_{substrate}$	1.5 mm		a	0.15
H	600 mm		W	4 mm
L	600 mm		W_m	100 mm
L_1	465 mm		L_2	70 mm

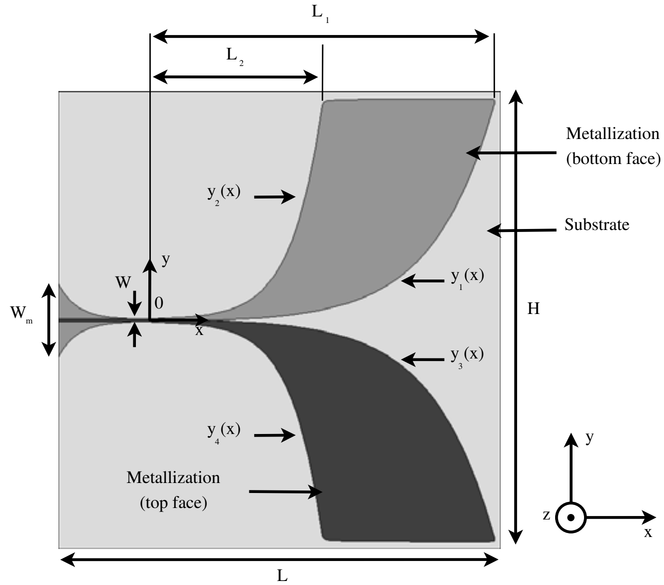

Figure 1. Geometry of the antipodal Vivaldi antenna with $a = 0.5$, $H = 600\,\mathrm{mm}$, $L = 600\,\mathrm{mm}$, $L_1 = 465\,\mathrm{mm}$, $W_m = 100\,\mathrm{mm}$.

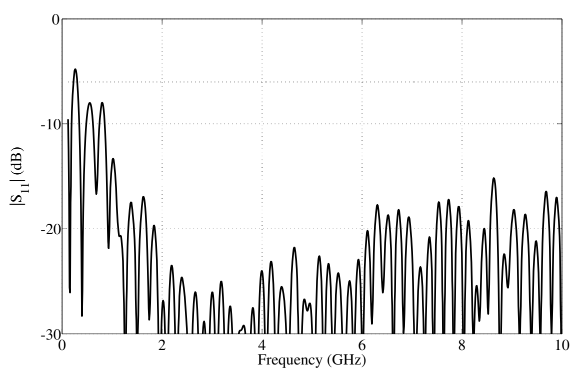

Figure 2. Reflection coefficient of the antipodal Vivaldi antenna with $a = 0.5$, $H = 600\,\mathrm{mm}$, $L = 600\,\mathrm{mm}$, $L_1 = 465\,\mathrm{mm}$, $W_m = 100\,\mathrm{mm}$.

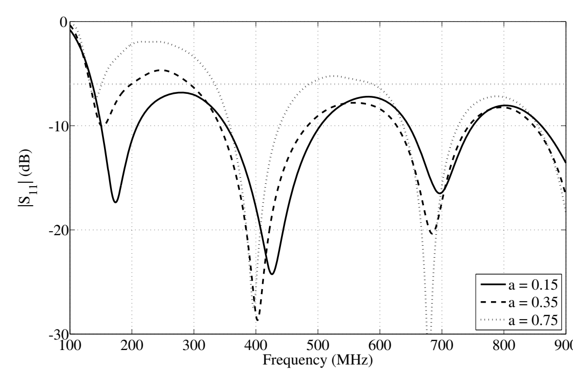

Figure 3. Influence of the coefficient a on the reflection coefficient on the lower band

2.3. Simulations under Flat and Bent Conditions

The simulations are carried out in the bandwidth of interest, from 100 MHz to 2 GHz. The impedance matching performances of the antenna under three bending conditions are compared with the performance in flat condition. The simulations are carried out with three radii of curvature R: 120 cm, 60 cm and 30 cm. Fig. 5(a) shows the antenna under the radius of curvature of 30 cm. Fig. 4 shows the influence of the three curvatures on the reflection coefficient and compared to the flat condition. As we can see, the curvatures do not affect the reflection coefficient up to 1 GHz. Between 1 GHz and 2 GHz the reflection coefficients are quite differents but are still under the threshold of $-6\,\mathrm{dB}$.

3. REALIZATION AND MEASUREMENTS

3.1. Fabrication Process

Figures 6(a) and 6(b) show the two sides of the antipodal Vivaldi antenna. The substrate is the characterized silicone-based one and the conductive parts are realized in an adhesive e-textile named

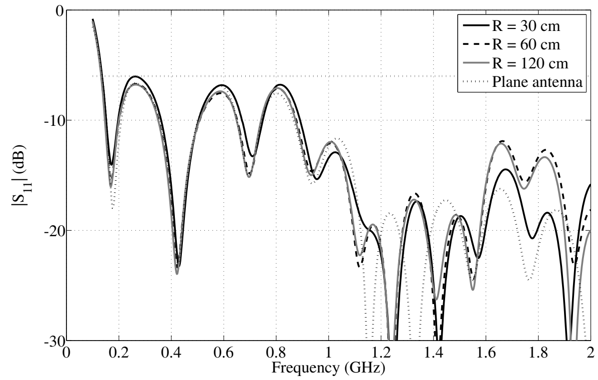

Figure 4. Simulated reflection coefficients of the antenna in flat condition and under three bending conditions.

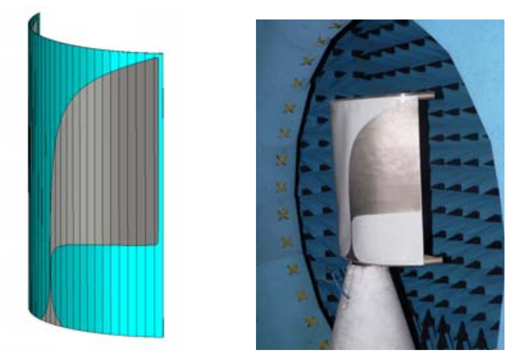

(a) (b)

Figure 5. Bent antipodal Vivaldi antenna.

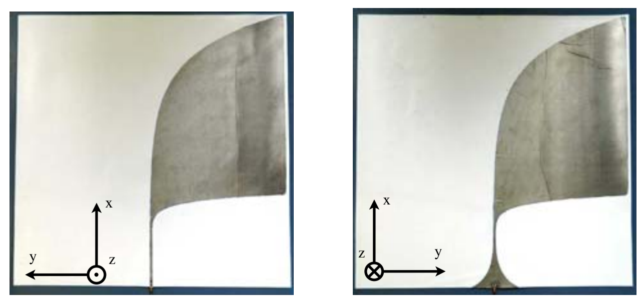

(a) Top face (b) Bottom face

Figure 6. Realized antipodal Vivaldi antenna.

Shieldit Super^{TM}. To carry out the measurements, a stiff-foam support is used to maintain the antenna, firstly in flat condition and secondly under a radius of curvature of 30 cm. The support is partially visible in Fig. 5(b).

3.2. Impedance Characterization

Figure 7 shows the measured reflection coefficient in flat condition and under a radius of curvature of 30 cm. As it can be observed, even if there are some slight differences from 1.1 GHz up to 2 GHz, the two reflection coefficients are quite similar. Moreover, in both cases the threshold of -6 dB is reached slightly below 150 MHz.

3.3. Radiation Patterns, Gains and Half Beamwidths

The measurements are carried out with a near-field measurement system SATIMO SG 32 (Fig. 5(b)). Due to the technical features of the system, the measurements start from 0.8 GHz.

The measured radiation patterns in the E-plane (xOy) are presented in Figs. 8(a), 8(b) and 8(c) respectively for 0.8 GHz, 1.5 GHz and 2 GHz, under flat and bent conditions, and compared to the simulated ones. Fairly good agreements can be observed between simulated and measured results. Moreover the behavior under both flat and curved conditions is similar.

The measured radiation patterns in the H-plane (xOz) are presented in Figs. 9(a), 9(b) and 9(c) for same frequencies and in the same conditions described above. The results between flat and bent antenna are in agreement for the main lobe but there are some differences in the side lobes. We can notice a depointing of the main lobe at 0.8 GHz (Fig. 9(a)) due to the bending of the antenna which is more important at this frequency than at 1.5 GHz or 2 GHz.

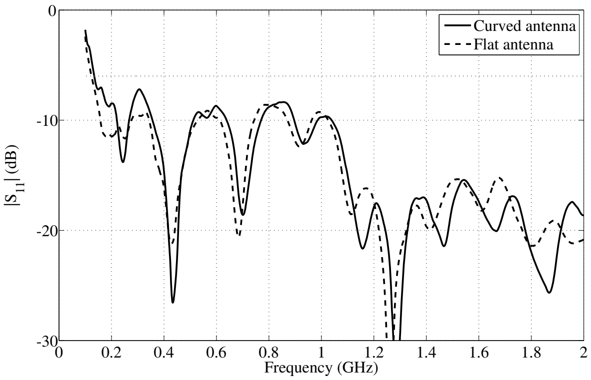

Figure 7. Measured reflection coefficients of the antenna in flat condition and with a radius of curvature of 30 cm.

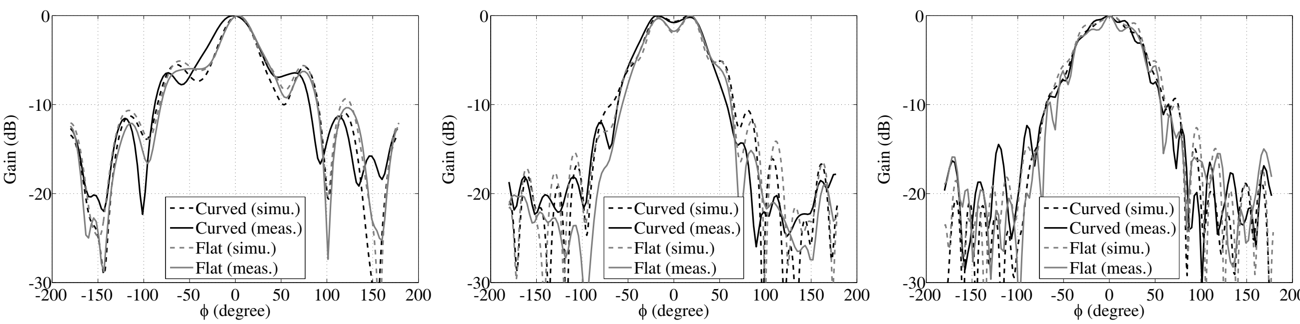

(a) 0.8 GHz (b) 1.5 GHz (c) 2 GHz

Figure 8. Simulated and measured normalized E-plane (xOy) radiation patterns.

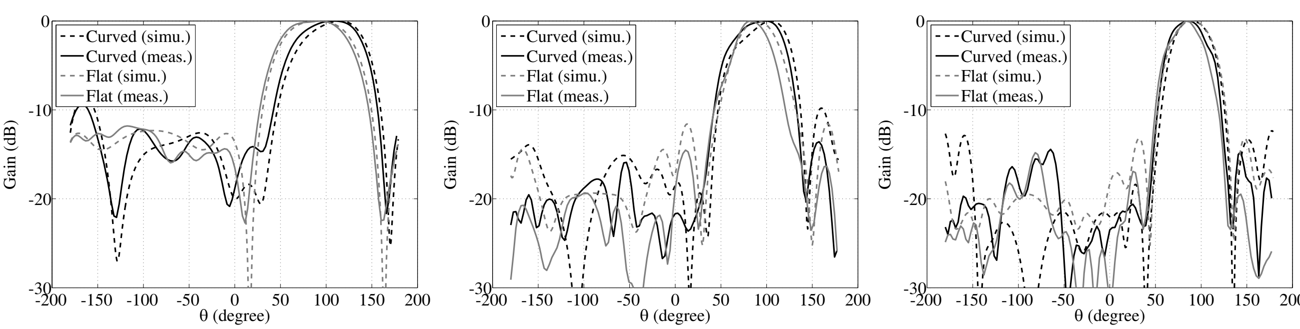

(a) 0.8 GHz (b) 1.5 GHz (c) 2 GHz

Figure 9. Simulated and measured normalized H-plane (xOz) radiation patterns.

The cross polar components, not represented to lighten the figures, are at least 20 dB lower than the co-polar ones.

The simulated half beamwidths, in flat and bent condition, for the (xOy) and (xOz) planes are presented in Fig. 10. In the (xOy) plane, from 0.1 GHz up to 0.3 GHz the half beamwidths are higher than the specifications. This phenomenon is due to the dimensions of the antenna which are smaller than the wavelengths of the frequencies included between 0.1 and 0.3 GHz. From 0.3 GHz up to 2 GHz the half beamwidths are around 60°. In the (xOz) plane, the half beamwidths decrease with the frequencies to reach 60° from 1 GHz. These results are in agreement with [5].

Figure 11 shows the maximum simulated and measured gain in the E-plane (xOy) for $\phi = 0^\circ$ from 0.8 GHz up to 2 GHz. As we can see on the simulated results, the curvature of the antenna does not

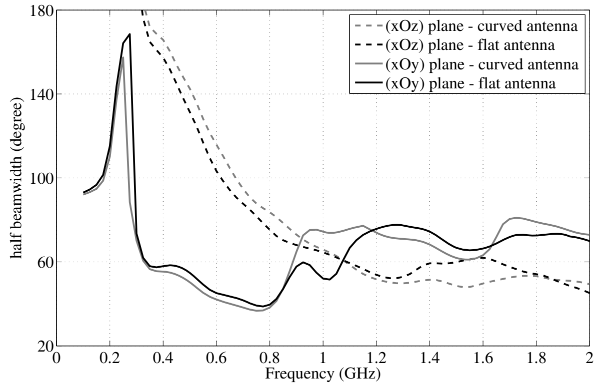

Figure 10. Simulated half beamwidth in the E-plane (xOy) and the H-plane (xOz).

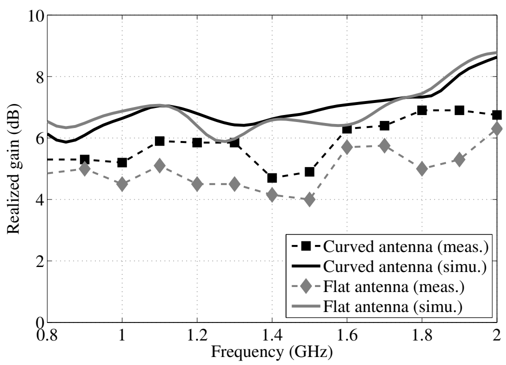

Figure 11. Maximum gains in the E-plane (xOy) and for $\phi = 0°$ for the antenna under flat and bent condition ($R = 30\,\mathrm{cm}$).

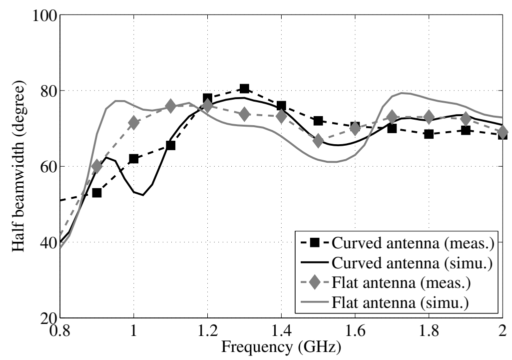

Figure 12. Measured and simulated half beamwidths in the E-plane (xOy) for the antenna under flat and bent condition ($R = 30\,\mathrm{cm}$).

affect the gain. This observation is also confirmed by the measurements. However, the measured gains are lower than the predicted values.

The half beamwidths from 0.8 GHz up to 2 GHz, deduced from the radiation patterns, are shown in Fig. 12. The two simulated results are similar except from 0.9 GHz to 1.2 GHz where the curved antenna is more directive. The measured results are in agreement with the simulations.

4. CONCLUSION

A flexible antipodal Vivaldi antenna has been designed and manufactured on a silicone-based substrate. To receive several signals in the VHF/UHF band, the realized antenna exhibits a -6 dB bandwidth from 150 MHz to 2 GHz. Some measurements have been carried out under plane and curved conditions to evaluate the performances of the antenna. These ones have shown that the antenna can be bent without alterations of the reflection coefficient, the half beamwidth and the gain. In the plane (xOy) the measured half beamwidths of the antenna are below 80° and are in agreement with the simulated ones. For $\phi = 0°$, the antenna presents a significant gain. The measured maximum gain is around 6 dB, slightly lower than the predicted result.

ACKNOWLEDGMENT

The authors wish to acknowledge the STAT (Section Technique de l'Armée de Terre — Versailles Satory — France) for the financial support and the Adjudant-Chef Christophe CAMUS for its technical guidance and supports.

APPENDIX A. THE ANTENNAS ON THE GAS BALLOON

Fig. A1 shows six identical antennas described in this papers placed under a gas balloon filled with helium. The receive signals are transmitted with a cable to the ground for signal processing.

(a)

(b)

Figure A1. Six identical antennas under a gas balloon during a test manipulation.

REFERENCES

1. Gibson, P. J., "The Vivaldi aerial," *9th European Microwave Conference, 1979*, 101–105, Sep. 17–20, 1979.
2. Shafieda, J. H., J. Noorinia, and C. Ghobadi, "Probing the feed line parameters in Vivaldi notch antennas," *Progress In Electromagnetics Research B*, Vol. 1, 237–252, 2008.
3. Shuppert, B., "Microstrip/slotline transitions: Modeling and experimental investigation," *IEEE Transactions on Microwave Theory and Techniques*, Vol. 36, No. 8, 1272–1282, Aug. 1988.
4. Shin, J. and S. H. Schaubert, "A parameter study of stripline-fed Vivaldi notch-antenna arrays," *IEEE Transactions on Antennas and Propagation*, Vol. 47, No. 5, 879–886, May 1999.
5. Gazit, E., "Improved design of the Vivaldi antenna," *IEEE Proceedings H — Microwaves, Antennas and Propagation*, Vol. 135, No. 2, 89–92, Apr. 1988.
6. Langley, J. D. S., P. S. Hall, and P. Newham, "Novel ultrawide-bandwidth Vivaldi antenna with low crosspolarisation," *Electronics Letters*, Vol. 29, No. 23, 2004–2005, Nov. 1993.
7. Mantash, M., S. Collardey, A.-C. Tarot, and A. Presse, "Dual-band WiFi and 4G LTE textile antenna," *2013 7th European Conference on Antennas and Propagation (EuCAP)*, 422–425, Apr. 2013.
8. Trajkovikj, J. and A. K. Skrivervik, "Soft and flexible antennas on permittivity adjustable PDMS substrates," *2012 Loughborough Antennas and Propagation Conference (LAPC)*, 1–4, Nov. 2012.
9. Liu, Q., K. L. Ford, R. Langley, A. Robinson, and S. Lacour, "Stretchable antennas," *2012 6th European Conference on Antennas and Propagation (EUCAP)*, 168–171, Mar. 2012.
10. Moon-Que, L. and N. Sangwook, "An accurate broadband measurment of substrate dielectric constant," *IEEE Microwave and Guided Wave Letters*, Vol. 6, No. 4, 168–170, Apr. 1996.
11. Liu, D., U. Pfeiffer, J. Grzyb, and B. Gaucher, *Advanced Millimeter-Wave Technologies: Antennas, Packaging and Circuit*, Ch. 5, 163–232, John Wiley and Sones, Ltd, UK, ISBN 978-0-470-99617-1, 2009.
12. Presse, A., J. M. Floc'h, A.-C. Tarot, and C. Camus, "Broadband UHF flexible Vivaldi antenna," *2013 Loughborough Antennas and Propagation Conference (LAPC)*, 277–280, Nov. 11–12, 2013.